Nanoscale

Chemical and Electrochemical Synthesis of Graphene Oxide - A Generalized View

Journal:	*Nanoscale*
Manuscript ID	NR-MRV-03-2020-002164.R1
Article Type:	Minireview
Date Submitted by the Author:	06-May-2020
Complete List of Authors:	Nishina, Yuta; Okayama University, Research Core for Interdisciplinary Sciences Eigler, Siegfried; Freie Universitat Berlin Fachbereich Biologie Chemie Pharmazie,

ARTICLE

Chemical and Electrochemical Synthesis of Graphene Oxide - A Generalized View

Received 00th January 20xx,
Accepted 00th January 20xx

DOI: 10.1039/x0xx00000x

Yuta Nishina,[a,b*] Siegfried Eigler[c*]

Graphene oxide (GO) is a water soluble carbon material in general suitable for applications in electronics, environment, or biomedicine. GO is yielded by oxidation of abundantly available graphite turning black graphite into water-dispersible single layers of functionalized graphene-related materials. Thereby, oxidation gives chemicals access to the complete surface area of GO. Those fundamentals led to a rich chemistry of GO. Here, we review the progress made in controlling the synthesis of GO, introduce the current structure models used to explain phenomena and present versatile strategies to functionalize the surface of GO. Finally, an outlook is given for future directions.

Introduction

In recent years, the research on GO increased enormously. Thereby, it is interesting to note that the number of papers related to GO increased within the last decade to about 3,500 research articles in 2019, as found by searching the key word graphene oxide at scopus.com. Thereby, the number of articles is outperforming those with solely graphene as key word. Although this simple consideration is very crude, it nevertheless shows that research on GO became extremely rich. The reason for the popular research on GO is because of the seemingly ease of synthesis, processing and chemical post-functionalization. While pristine graphene is limited in processability, GO is more versatile and thus opens complementary and interdisciplinary fields of research.

GO can be applied in various fields of research, allowing the engineering of materials properties. The discovery of the properties of graphene accelerated the research on GO, however, now research on GO became a research area on it own.

The research results on GO regarding synthesis or applications were summarized in various review articles, some of which are cited here.[1-15] A very recent overview is given by Brisebois and Siaj.[16] Here, we want to give a more generalized view on the synthesis of GO and present generalized approaches. Moreover, we introduce recent strategies for post-functionalization. In addition, we give advice for reliably characterizing GO materials to encourage researchers of all disciplines to derive structure-property relations in future research.

GO is currently applied in various applications and here we direct to recent research papers or recent review articles. The mentioned applications are no limitation nor are those a complete list. Main fields of research of GO are transparent conductive films,[17] strong and stiff papers,[18] fibers,[19] aerogels,[20] separators of pollutants,[21] membranes,[22] energy storage devices,[23, 24] sensing,[25] luminescent materials,[26] lithium-ion batteries,[27] fuel cells,[28] biomedicine,[29] liquid crystals[30] and polymer composites.[31]

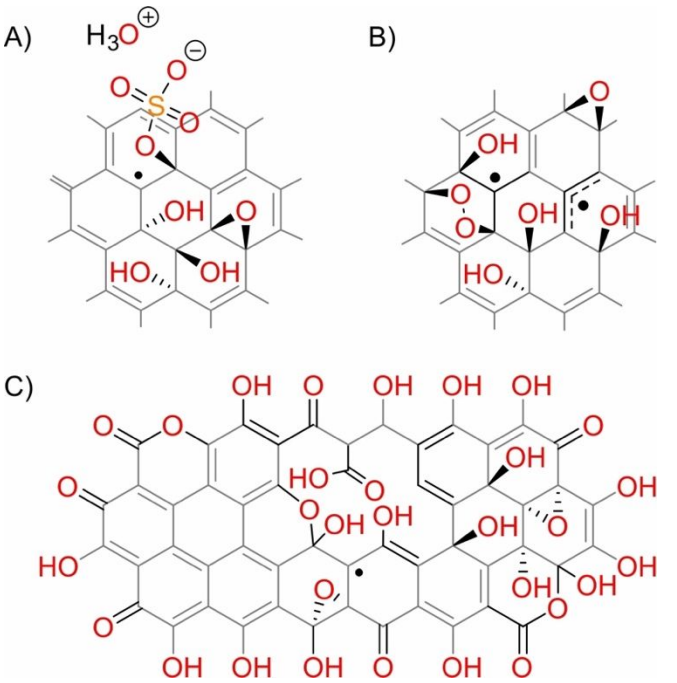

Figure 1. A) Generalized chemical sketch of GO, not accounting for defects or functional groups at rims of flakes. Model includes: π-system, hydroxyl and epoxy groups, organosulfate groups, and carbon radicals. B) Chemical sketch of GO accounting for radical structures, such as carbon centred or allylic radicals and cell toxic endoperoxide groups. C) Chemical sketch of GO accounting for π-system, butadiene structures, hydroxyl and epoxy groups and functional groups at defect sites and rims of flakes with phenol-like, carbonyl, hemiacetal, or lactol structures.

[a.] *Graduate School of Natural Science and Technology, Okayama University Tsushimanaka, Kita-ku, Okayama, 700-8530, Japan; e-mail: nisina-y@cc.okayama-u.ac.jp*
[b.] *Research Core for Interdisciplinary Sciences, Okayama University Tsushimanaka, Kita-ku,Okayama,700-8530, Japan.*
[c.] *Institute of Chemistry and Biochemistry, Freie Universität Berlin, Takustraße 3, 14195 Berlin, Germany; e-mail: siegfried.eigler@fu-berlin.de.*

Generalized synthetic view on the synthesis of graphene oxide

The synthesis of GO goes back to the experimental work described in 1840,[32] and in 1855 a reliable method was described to turn black graphite to yellowish GO.[33] The fascinating oxidation product GO arose attention of several researchers in the following 165 years, and new methods were presented leading to yellowish GO.[34-38] However, modern analytical techniques were necessary to reveal the structure of GO, a prerequisite to explain experimental observations. Other review articles and books give deep insights into the research on GO between roughly 1840 and 2000 and beyond, as they are cited in this introduction. Here, we give a generalized overview on the synthetic approaches leading to GO, including chemical oxidants and electrochemical methods.

Structure models of GO. The Lerf-Klinowski model,[39] which is based on solid-state NMR spectroscopy, describes GO as a material with randomly distributed epoxy-groups (1,2-ethers, 60 ppm) and hydroxyl-groups (70 ppm), in addition to aromatic sp^2-patches (130 ppm), compare **Figure 4**. The model was confirmed by NMR studies of Ishii, giving more detailed insights.[40, 41] Structural models, accounting for different kinds of properties and functional groups are depicted in **Figure 1A-C**. Carbon centered radicals are reported,[42] which are presumably present in any kind of GO, however, also allyl radicals are plausible (**Figure 1B**). Moreover, endoperoxide groups were identified, which are determining cell toxicity.[43] Dimiev et al. introduced the dynamic structure model (DSM) of GO,[44, 45] which also explains the degradation of GO (**Figure 2**). In general, the more defects are introduced into the structure of GO, as a consequence of overoxidation and accompanied formation of CO_2, the more complex the structure of GO becomes. Consequently, any kind of functional group containing oxygen is reported, as summarized in a recent review article.[16] Thus, lattice defects and the functional groups at those rims may determine the properties of GO and therefore differing properties have been reported. A structure model accounting also for defects is given in **Figure 1C**. Accordingly, with introducing vacancy defects, the rims of flakes and rims within the flake at defect-sites may be functionalized by carboxylic acids, phenol-like hydroxyl groups, hemiacetals, lactones, lactols or ketones. The shown model is not accounting for structures with extended defects and the accompanied rearrangement of the carbon framework such as five, seven or larger rings, in addition to nm-sized holes.

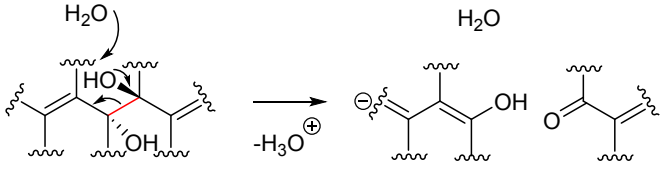

Figure 2. The DSM model of GO. Deprotonation of vicinal diols of GO by water leads to C-C bond cleavage and the formation of acidic enol groups and carbonyl groups.[46]

Moreover, in the course of strong overoxidation, small carbon patches may be cleaved from flakes and become highly oxidized what leads to the formation of oxidative debris,[47, 48] and those highly oxidized fragments may adsorb to the surface of GO flakes. Taking all possibilities into account, GO is defined as a sheet-structured material with oxo-functional groups.

In the following we describe and discuss steps of the synthesis of GO, which can be distinguished.

Graphite as starting material. In general, any source of graphite can be used for the oxidation to GO, such as graphite with ordered layers, or expanded graphite (**Figure 3A**). However, graphite materials differ in the size of flakes, density of defects, and crystallinity.[49] Since GO is composed of flakes, the maximum lateral dimensions of flakes of GO are limited to the grain-size of graphite (**Figure 3A**). In this regard, applications based on large flakes of GO should start with a source of graphite with large grain, while applications, based on flakes that require nm-sized flakes may better use an appropriate graphite with smaller grain. It is described in the literature that the lateral dimensions of flakes of GO can be comminuted e.g. by sonication.[50-52] Thus, it is plausible that flakes break at grain boundaries during oxidation, work-up or by sonication.

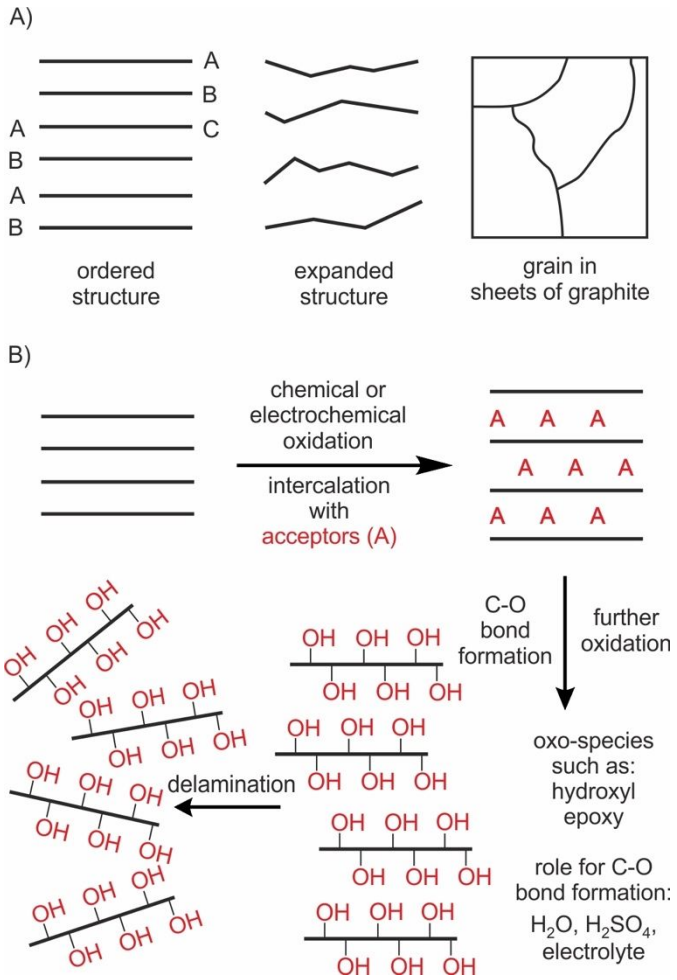

Figure 3. A) Illustration of graphite source with different crystallinity, order and grain-size. B) Generalized illustration of the oxidation of graphite, involving: intercalation of electron acceptors forming graphite intercalation compounds (p-doping of graphene sheets), further oxidation leads to the formation of C-O bonds Intercalation and subsequent oxidation by O-transfer occurs often simultaneously within one graphite particle, however, these processes depend on the reaction conditions. Thereby, oxidants, water, sulfuric acid/nitric acid or electrolyte play a decisive role.

Not only flakes of graphite are used, but also graphite rod electrodes, highly-oriented pyrolytic graphite (HOPG), kish graphite, or foils of graphite produced by compression of expanded graphite or pyrolysis of polyimide can be used as a source of GO. A bottleneck using graphite rod electrodes is that they tend to break upon electrolysis, and multi-layered materials are produced. A similar phenomenon occurs when compressed graphite sheets are used. In contrast, highly crystalline foils of graphite do not undergo in plane cleavage, allowing continuous production of GO, as introduced later.

Electronic oxidation (p-doping) of graphite by the oxidant. In general, oxidation is defined by the release of electrons or, if oxygen is involved, oxygen atoms are taken up. For the process of GO synthesis, graphite becomes first p-doped or electronically oxidized up to a density of charge carriers approaching $1.6x10^{14}$ cm^{-2} for hole carriers, taking into assumption that an intercalation compound, such as graphite sulfate is formed, which consists in first approximation of C_{24}^{+}-subunits with hydrogensulfate counter-ions and sulfuric acid molecules placed at the residual lattice spaces (**Figure 3B**).[53] This kind of p-doping leads to the formation of e.g., stage 1 graphite sulfate and can be achieved by chemical oxidation in bulk quantities. [54, 55] However, electrochemical methods not only allow the synthesis of stage 1 graphite sulfate, but also give control over staging, as summarized in the literature.[53, 56-58]

Functionalization of the carbon framework by oxo-addends. In general, with p-doping graphite intercalation is enabled. However, the presence of strong oxidants or applying higher potentials leads to the formation of C-O bonds and thus, graphite oxide is formed (**Figure 3B**).

In the case of chemical oxidation, a potent oxidant must be used, and the most often one used is potassium permanganate, which most likely forms Mn_2O_7 in acidic reaction mixtures. However, up to now, the degree of oxidation can only be speculated on. With oxidation, Mn-species intercalate into the galleries of the graphite intercalation compound, such as graphite sulfate. The driving force for taking up Mn-species is however not fully understood. In this context, Mn_2O_7 may displace H_2SO_4 or if Mn_2O_7 is considered as ion pair, MnO_3^{+} and HSO_4^{-} could form a new ion pair forcing the exchange of HSO_4^{-} by MnO_4^{-} in graphite sulfate. Since MnO_4^{-} is a strong oxidant the carbon framework is further oxidized and this may occur by electron transfer to intercalated Mn-species or also to Mn-species outside the galleries. However, this process is not fully understood. Pristine graphite oxide was introduced in the literature, which possesses carbon layers covalently functionalized by C-O-S bonds described as cyclic organosulfate groups.[44] However, also C-O-Mn-species are plausibly formed. Experimental investigations clearly show that Mn^{VII} is transformed to Mn^{III} with graphite oxide formation.[59] Subsequently, H_2O_2 is added to the reaction mixture to solubilize Mn-species. Next, the sulfuric acid is hydrolysed and temperatures of 98 °C are described by Hummers and Offeman.[38] However, such a high temperature may alter the properties of GO and lattice defects may be introduced.[60] Also, low temperature hydrolysis of sulfuric acid is described at temperatures < 10 °C.[61] With the addition of water, it can be assumed that C-O bonds stemming from water are formed, however, ^{18}O tracing experiments did not find evidence that oxygen in GO stems from water in chemical oxidation.[59] In contrast, ^{18}O tracing experiments conducted for the electrochemical oxidation of graphite in aqueous sulfuric acid suggests that oxygen in GO stems from water.[62] Therefore, the origin of oxygen of GO can be different for chemical and electrochemical oxidation, respectively.

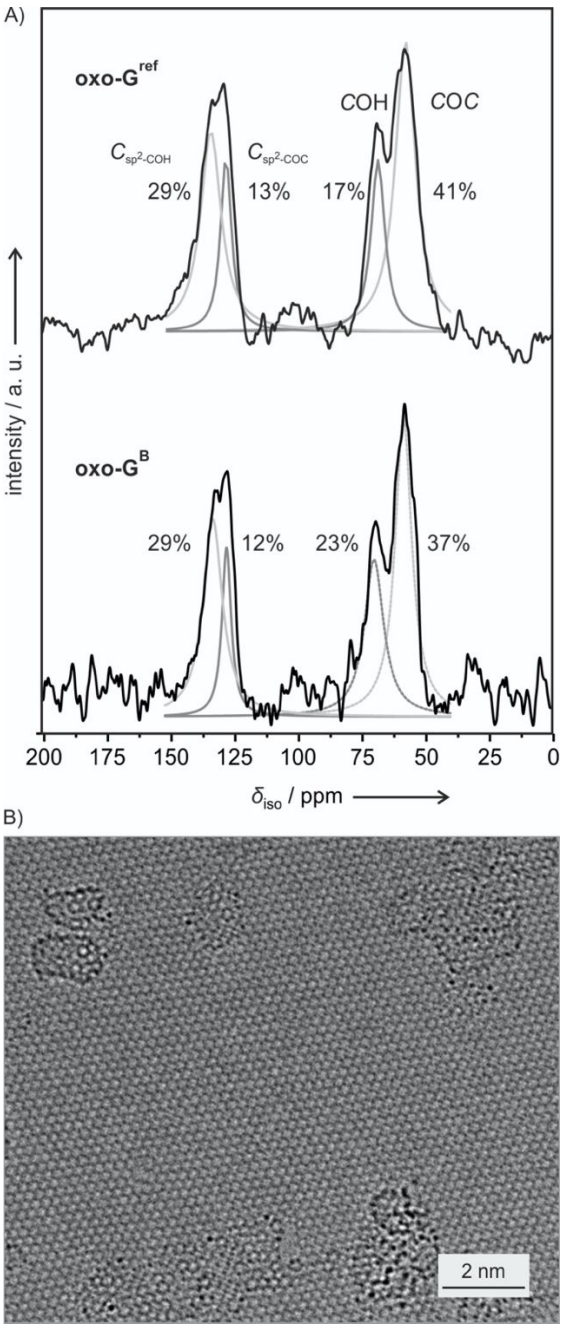

Figure 4. A) Nuclear magnetic resonance spectra measured in solids of oxo-G^{ref} and oxo-G^{B}, respectively. B) Cc/Cs-corrected high-resolution 80 kV TEM image of graphene derived from oxo-G^{ref}. Reproduced with permission from Wiley-VCH.[63]

Modified methods of the synthesis of GO by chemical oxidation. In the literature, there are diverging reports on the necessary amount of reagents, such as potassium

permanganate or additives. Those reports are all described as "modified Hummers' method" or "improved Hummers' method" or similar.[64] In the original experiment described by Hummers,[38] which is basically the same as described by Charpy in 1909,[36] 3 g (19 mmol) of potassium permanganate are used to oxidize 1 g (83 mmol) of graphite (molar ratio of carbon/$KMnO_4$ = 4.37).

Although Mn-redox chemistry is quite complex, Mn^{3+} is mainly formed and thus, up to four electrons (76 mmol, molar ratio of carbon/electron = 0,92) can be accepted by using 3 g of $KMnO_4$ as oxidant.[59] With the described amount of permanganate, a degree of functionalization of up to about 90% could be achieved in theory. Following those considerations, about 2 g of $KMnO_4$ (molar ratio of carbon/electron = 0,61) would be sufficient to oxidize 1 g of graphite to achieve a degree of functionalization of about 60%. However, higher amounts of oxidant are necessary to overcome activation barriers, depending on the crystallinity of graphite and thus, in practice 3 g are most often used. As recently determined, the friction of intercalated species plays an important role for intercalation and imperfections may stop intercalation and require higher oxidation potentials.[54] Thus, we conclude that the type of graphite plays an important role.

Chlorate as alternative oxidant. The method described by Brodie involves mixing of graphite with sodium chlorate and subsequent treatment by nitric acid.[33] This type of oxidation is repeated several times, however two or three repetitions may be enough to allow complete delamination to form GO.[63] Thereby, nitric acid reacts with chlorate forming gaseous ClO_2, which however was described to potentially accumulate and detonate at temperatures of roughly 40 °C. Therefore, the method is much less often used, compared to oxidation protocols using potassium permanganate. Nevertheless, the oxidation process of graphite by Brodie method is kinetically limited, because of phase transfer processes.[63] Here, the intercalation compound graphite nitrate is formed (liquid/solid interface facilitating oxidation) and ClO_2 facilitates further oxidation (gas in liquid, oxidizing solid graphite). Although, the preparation process differs from the oxidation described by Hummers', we recently demonstrated that the surface functional groups are practically the same as for oxo-G prepared by permanganate oxidation (**Figure 4A**).[63]

Delamination of graphite oxide to form graphene oxide. Although the graphite oxidation product is mostly termed as GO, first graphite oxide is formed, which consists of stacks of single layers of GO. Delamination is achieved by sonication, as a general method. However, sonication is not needed, since delamination of single layers of GO proceeds also once the ionic strength is reduced and even a 1/1 mixture of water and methanol leads to delamination.[65] From experience, we find that swelling proceeds with washing steps, which can be a problem using filtration to remove the sulfuric acid.

Here, we want to point to problems in scale-up. While 1 g of graphite can easily be produced in a small flask of 250 ml volume, work-up requires several liters of pure water for washing. For delamination to single layers the concentration is reduced to below 1 mg/ml, better 0.1 mg/ml. After purification in diluted conditions, flakes of GO can be concentrated by centrifugation, keeping the high purity. This process already requires a large centrifuge and makes clear that scale-up to the 10 g or kg-scale requires either special techniques or contaminants remain in the product.

There is no standard procedure for the purification of GO, however, washing by HCl, centrifugation and redispersion in pure water are commonly used.[66] In the case of repeated centrifugation and redispersion, it is important to allow swelling after redispersion, because this process needs time. Finally, a pH of about six to seven is reached and graphite oxide delaminates to single layer flakes by simple shaking. In addition, washing of delaminated GO by diluted H_2O_2 makes sense to remove manganese salts further, which may have been trapped between layers of graphite oxide. Avoiding sonication steps preserves large flakes of GO, which otherwise break upon sonication treatment in dependence of the energy input.[50, 52]

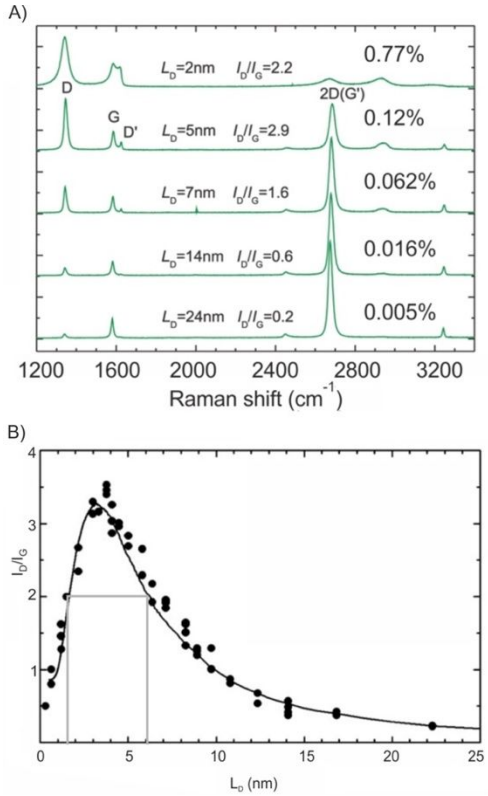

Figure 5. A) Individual Raman spectra of graphene with different densities of defects between 0.005% and 0.77%, respectively. Adapted with permission from American Chemical Society.[67] B) Plot of the I_D/I_G ratio against the distance of defects, which is following a relation. Reproduced with permission of Elsevier Ltd.[68]

Determination of the purity of graphene oxide. The above described chemical oxidation of graphite is quite convenient and can be accomplished within a week or two depending on the needed purity , amount or quality of GO. Thereby, GO can be prepared on the g-scale what is enough for laboratory experiments. Thermogravimetry measured up to 800 °C under inert conditions gives evidence, whether GO bears organosulfate groups or not, because those decompose between 250 °C and 300 °C. With the presence of inorganic sulfate impurities, little weight-loss between 250 °C and 300 °C

occurs in addition to the weight-loss between 700 °C and 800 °C. XPS can be used to determine the C/O ratio, or to investigate contaminants. In particular, Mn^{2+} can be identified by EPR and if present washing by HCl, water or aqueous EDTA (ethylenediaminetetraacetic acid disodium salt) can remove Mn^{2+}.[43] If the catalytic activity of GO derived materials is in the focus of research, also ICP-OES or ICP-MS should be performed to search for trace amounts of metal impurities.[69]

Determination of the quality of graphene oxide. The term quality used in the context of GO may have differing meaning and may relate to a defined surface chemistry, purity or integrity of the carbon framework. In the case of electronic applications, the quality of the hexagonal carbon framework is decisive.[61, 70] The best way to quantify defects in GO is to measure Raman spectra of single layers of reduced GO. Raman spectroscopy can be used to determine the average distance of lattice defects at 532 nm excitation wavelength.[67, 68, 71, 72] Typically, a film of monolayer flakes is deposited on Si/300 nm SiO_2, e.g. by Langmuir-Blodgett technique, or alternatively by immersing a substrate in a diluted aqueous dispersion of GO. Subsequently, chemical reduction by vapour of a 1/1 volume ratio of hydriodic acid and trifluoro acidic acid can be used to quantitatively remove oxo-addends from the carbon framework to restore graphene. The reduction of GO is rapid and after few minutes the reduction can be assumed to be complete. We recognized that annealing at 140 °C can improve the adhesion of flakes to the substrate, enabling washing the surface at room temperature with water avoiding scrolling of flakes to remove adhering iodine species. Subsequently, statistical Raman spectroscopy can be conducted, either automated by mapping or by measuring a set of individual monolayer flakes, e.g. 300 flakes. The I_D/I_G ratio can be related to the distance of defects following the rationale analysis introduced by Lucchese and Cançado (**Figure 5**).[67, 68] However, once a density of defects of 1% or higher is reached, the I_D/I_G ratio saturates. Consequently, the Raman ID/IG ratio is not a measure to characterize GO, and chemical reduction is necessary to conclude on the degree of defects already present in GO.

With regards to densities of defects produced by standard oxidation protocols for the synthesis of GO, it can be estimated that about 1 CO_2 molecule is formed on 20 carbon atoms (density of defects: 5%).[44] In addition, the formation of CO_2 during the oxidation process was further investigated at different temperatures.[59] While at 10 °C no CO_2 formation was observed, about 0.06% of carbon are oxidized at 35 °C and 3.5% at 80 °C (2 h reaction time using C/$KMnO_4$ ratio of 1/3). The density of defects may however be higher in the final product of GO, since more CO_2 is likely produced during aqueous work-up, involving hydrolysis of concentrated sulfuric acid, a process accompanied by the formation of heat. However, temperature control can improve the quality substantially.[61]

For determining the density of defects in graphene type materials, such as reduced GO, which bears too many defects to use the I_D/I_G ratio as a measure, a Raman spectroscopy-based method was described that makes use of the variation of the Raman cross section, which is dependent on the density of defects. It was found that the measured intensity of the D or G band (**Figure 6**),[73] scales linearly for densities of defects between 0.1% and 30% on double logarithmic scales and thus, allows determining densities of defects of several %. To apply this method successfully, it is important to probe single layers of deposited GO, as multi-layers or folds will increase the Raman intensity thus overestimating the density of defects. The results are in first approximation also supported by transmission electron microscopy (TEM) at atomic resolution.[74] In **Figure 4B** a TEM image at atomic resolution is depicted for a certain high quality of GO with very few defects.[63]

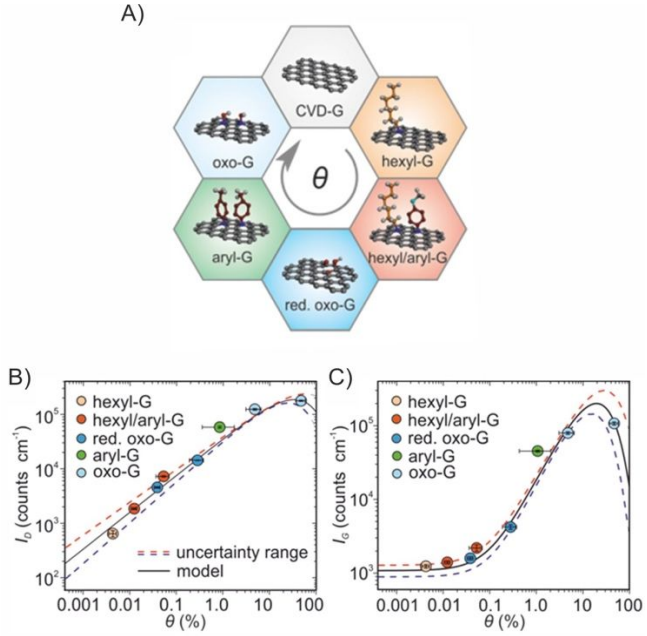

Figure 6. A) Illustration of derivatives of graphene with increasing density of vacancy defects and functionalization defects, respectively. B) Plot of the intensity I_D against the density of defects. C) Plot of the intensity ratio I_D/I_G against the density of defects. Reproduced with permission from Springer Nature.[73]

Kinetically controlled synthesis of graphene oxide. Keeping the density of lattice defects in GO below 1% requires kinetic control over the oxidation reaction, which was demonstrated by following different strategies, such as keeping the degree of oxidation on the p-doping level of about 4%, as in graphite sulfate.[54] In that approach, the average density of defects could be minimized to 0.02%.[54] Alternatively, kinetic control of oxidation was achieved by lowering the oxidation temperature < 10 °C.[61] That approach leads to densities of defects of about 0.4% in average. Also interface controlled oxidation, as in the case of chlorate oxidation can be conducted and densities of defects of about 0.07% in average were determined.[63] Those materials, which allow determination of the density of defects by interpreting the I_D/I_G ratio are GO materials where defects play a minor role e.g., for chemical transformations and thus, oxo-addends are in majority attached to both sides of the hexagonal carbon framework, instead of defect-sites. Those materials are better described as graphene with oxo-addends and were termed as oxo-functionalized graphene (oxo-G).[15]

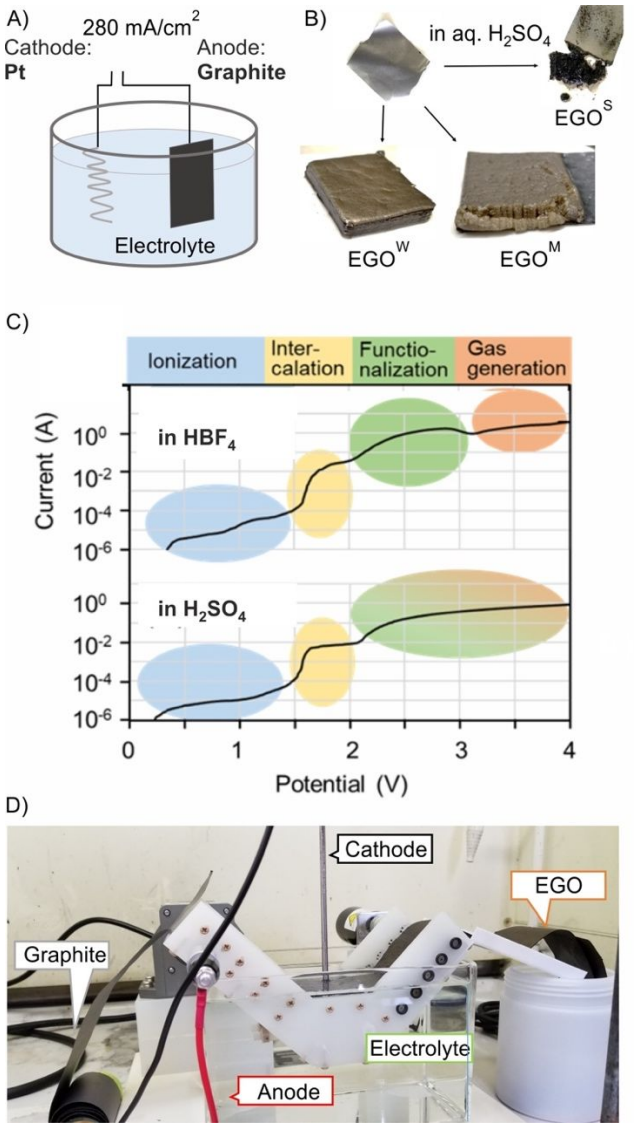

Figure 7. Illustration of the electrochemical oxidation of graphite, in particular graphite foils. A) Illustration of the electrochemical preparation setup. B) Photograph of a graphite foil and the oxidation products with sulfuric acid, a mixture of HBF_4 and water and HBF_4 and methanol as electrolyte, respectively. C) I/V potentiostatic plot illustration the steps of the electrochemical oxidation. D) Photograph of the setup of the continuous anodic oxidation of a roll of graphite leading to a foil of GO, which is subsequently purified. Reproduced with permission of Elsevier Ltd..[75]

Electrochemical oxidation of graphite. Chemical oxidation approaches suffer from time-consuming procedures, need of well-controlled operating-temperatures, and aggressive reagents; all of which result in relatively high costs of GO when industrially scaled up. However, electrochemical approaches to graphene materials have gained significant attention to solve the above issues.[76, 77] At the anode, graphite oxidation proceeds. In contrast, at the cathode, reduction proceeds. Further, anion intercalation occurs at the anode, and cation intercalation occurs at the cathode. Here, we focus on the anode oxidation of graphite to produce GO. Anodic graphite oxidation reactions have been investigated and results were published since 1930s, and developed tremendously in recent years.[78-80] In electrochemical approaches, the oxidation potential can be regulated giving control over the oxidation process. In addition, no oxidant is needed and therefore, certain impurities are avoided. In general, the electrochemical oxidation proceeds in analogy to the chemical oxidation of graphite. Accordingly, first intercalation takes place, followed by covalent bond formation (oxidation) (**Figure 7C**). Similar to the chemical oxidation, various graphite sources, such as rods, powdesr, foisl, and HOPG, can be used. The connection of graphite with a current collector is crucially important to oxidize uniformly. Therefore, graphite powders are converted to few-layered GO (graphite oxide) and not a single layers.[81] Here, we highlight a method that leads to uniform oxidation of graphite, utilizing a graphite-foil using na electrolyte that plays a crucial role for facilitating intercalation and functionalization. Conventionally, H_2SO_4 or its salts have been used as an electrolyte,[62] however, SO_4^{2-}-type electrolytes promote the formation of gas, possibly O_2 from water, to break graphite anodes during the electrolysis (**Figure 7A, B**). To suppress the formation of gases, stable anions, such as BF_4^- or PF_6^- have recently been employed, enabling uniform and continuous roll-to-roll production of GO (**Figure 7D**).[75] It is still not clear, but we now consider the activation of water co-intercalated with BF_4^- or PF_6^- is more efficient than SO_4^{2-} systems, forming oxy and hydroxy radicals closer to the graphene layers. A small polar organic solvents, such as methanol, ethanol, and acetonitrile can be used in combination with the water/BF_4^- system. The addition of the organic solvent promotes a more uniform expansion and oxidation of the graphite sheet, possibly because of further suppressing the formation of gas from water. Although a lot of progress was made, and mechanistic ideas can up, futher investigations can still lead to improved reactivity leading to more uniform materials.

In situ or post-functionalization of graphene oxide. The synthesis of GO suffers from batch to batch variations due to variable rotation speed, differing sources of graphite or varying local temperatures during oxidation and work-up. Moreover, during work-up the practice of centrifugation and redispersion processes may vary, or sonication time, if applied. The consequence is that impurities of reagents remain part of GO on the one hand, and on the other hand work-up conditions may change the surface chemistry or even decompose the carbon lattice by C-C bond breaking.

With using sulfuric acid for the synthesis of GO, organosulfate groups may be formed, in particular keeping low temperatures.[82] However, during work-up, the oxidation mixture is often mixed with water, which leads to an increase of the temperatures to more than 90 °C. At such temperatures, organosulfates are however hydrolysed.[83] Also, the treatment of GO by HCl may cleave organosulfate, in particular at elevated temperatures, such as 40 °C (**Figure 8**). Consequently, after the synthesis of GO, subsequent reactions can be applied to modify the chemistry of the initial GO. Thus, the degree of functionalization of GO can be adopted by e.g. partial reduction of GO using defined amounts of reducing agents. We note that the degree of oxidation can, to some extent, be adjusted, either by the oxidation protocol (in particular using electrochemistry) or by post processing. Also adjusting the pH value influences the

surface chemistry of GO. We demonstrated that base treatment at a temperature of 10 °C leads to partial cleavage of epoxy groups forming hydroxyl groups in majority and if present organosulfate groups are cleaved.[83] In addition, there is strong evidence that base treatment induces the rearrangement of on-plane functional groups, which otherwise proceeds very slow, as found by nucleotide binding studies.[84]

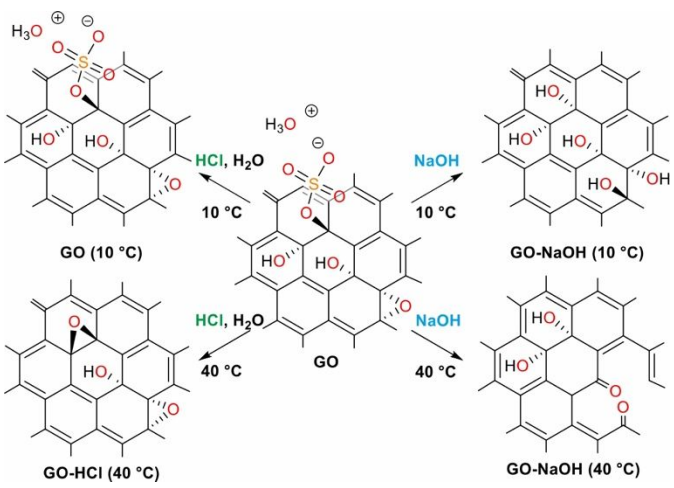

Figure 8. Chemical sketch of GO with hydroxyl, epoxy and organosulfate groups, which can undergo chemical transformations depending on the reaction condition. Those reaction conditions can be applied during the work-up of GO what leads to different graphene derivatives. Reproduced with permission from The Royal Society of Chemistry.[83]

At elevated temperatures, such as 40 °C and a pH value of roughly 9, defects are introduced into the carbon lattice what may even lead to the disintegration of flakes of GO.[85] Moreover, it was reported that treatment of GO by base leads to reductive defunctionalisation of oxo-addends.[16, 86] Although hydroxide is not a potent reducing agent, it is plausible that the electron affinity of GO is locally high enough for electron transfer processes, in particular at patches, which are highly functionalized.

Strategies to functionalize graphene oxide

Methods for the chemical modification of GO utilizes oxygen functional groups (**Figure 9**). Esterification or amidation is achieved by converting the carboxyl groups on GO (Equation I, **Figure 9**); however, in our experience, the reaction does not proceed sufficiently. This would be because GO does not contain many carboxyl groups. In this context, it was found by temperature programmed desorption up to 1800 °C that hydroxyl groups cover rims of flakes in majority.[87] As for the conversion of the hydroxyl groups on GO, etherification or esterification can be considered (Equation ii, **Figure 9**), but esterification is also limited.[88] The most commonly used functionalization method is a nucleophilic addition reaction of epoxy groups. An amine can be reacted with the epoxy group on GO, and the Kaiser test can evaluate the immobilized amount (Equation iii, **Figure 9**).[88] Recently, the formation of an onium bond is developed by halogen activation of GO, followed by the treatment with an amine (Equation iv, **Figure 9**) leading to an efficient chemical modification.[89]

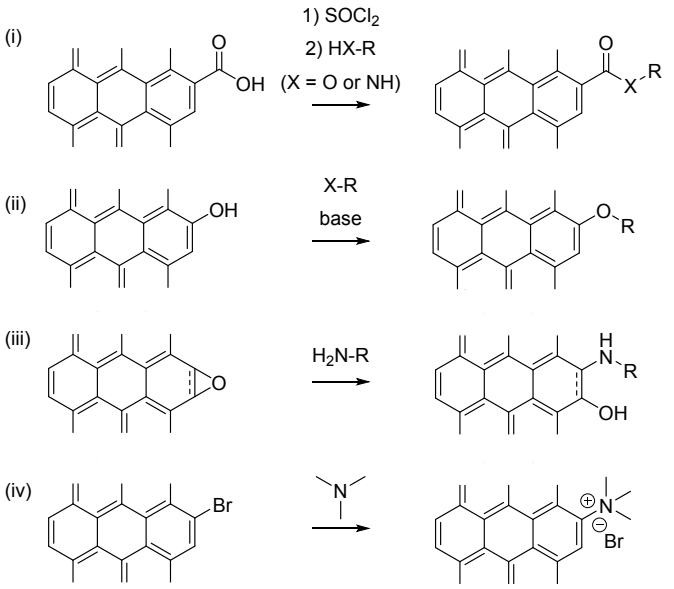

Figure 9. Illustration of chemical transformation strategies for the functionalization of GO and reduced GO, respectively, involving esterification, amidation, etherification, opening of epoxy groups by amines or halogenation and substitution by amines.

Conclusions

The observation of the conversion of black graphite to yellowish material that can be termed graphene oxide appears to be too simple. In particular, the chemical structure of GO must be resolved to minimize the chemical uncertainty. In general, defects in terms of a ruptured carbon framework may determine the structure and properties of GO, however, the vacancy defects can also be minimized. Functional groups on the basal plane of GO are hydroxyl and epoxy groups. In addition, other functional groups, such as organosulfate may be present, in dependence on the preparation conditions or post-functionalization, which also occurs during work-up. Thus, it can be concluded that properties of GO depend on the preparation protocol and the chemical structure must be determined for individual processes.

The synthesis of GO generally proceeds by intercalation, followed by covalent bond formation. As a side reaction, which may also become dominant, carbon-carbon bonds break and CO_2 forms leading to complex chemical structures and the formation of holes. Consequently, not only the rims of flakes, but also the rims of holes may become functionalized by oxo-groups, such as carbonyl, carboxyl, or phenol-like groups. Thus, in consequence of extrented oxidation, also oxidative debris, a humic acid-like material, may be produced with any kind of oxo-functionality.

Control over the oxidation process is possible, however, carefully chosen reaction conditions are necessary. Virtually, any potent oxidant, including electrochemical potentials, can be used for the activation of graphite. However, acceptors with the ability to form intercalation compounds are necessary to activate all layers of graphite. Subsequently, further oxidation and covalent bond formation must be controlled without

causing overoxidation, which would lead to CO_2 formation. Up to now, chemical and electrochemical methods are available to form GO, however, multi-layer formation remains problematic, but can be overcome by choosing the right graphite source, preparation, and work-up protocol.

With access to the complete surface of GO, chemical post-functionalization is possible and advanced approaches are introduced in this review. However, the degree of functionalization must be determined individually and the performance in application cannot be predicted.

It can be concluded that post-functionalization of GO can improve the performance of any kind of applications mentioned in the introduction. For furture directions of the synthesis of GO, we conclude that electrochemical methods will further develop to provide highly pure GO, produced on a large scale with defined surface chemistry.

Conflicts of interest

There are no conflicts to declare.

Acknowledgements

This research is supported by the Deutsche Forschungsgemeinschaft (DFG, German Research Foundation), project number 392444269, and JST CREST, project number JPMJCR18R3.

References

1 S. F. Kiew, L. V. Kiew, H. B. Lee, T. Imae and L. Y. Chung, *J. Control. Release*, 2016, **226**, 217-228.
2 O. C. Compton and S. T. Nguyen, *Small*, 2010, **6**, 711-723.
3 Y. Zhu, S. Murali, W. Cai, X. Li, J. W. Suk, J. R. Potts and R. S. Ruoff, *Adv. Mater.*, 2010, **22**, 3906-3924.
4 Y. Wang, Z. Li, J. Wang, J. Li and Y. Lin, *Trends Biotechnol.*, 2011, **29**, 205-212.
5 K. Toda, R. Furue and S. Hayami, *Anal. Chim. Acta*, 2015, **878**, 43-53.
6 R. J. Young, I. A. Kinloch, L. Gong and K. S. Novoselov, *Compos. Sci. Technol.*, 2012, **72**, 1459-1476.
7 J. Liu, L. Cui and D. Losic, *Acta Biomater.*, 2013, **9**, 9243-9257.
8 Y. Zhu, D. K. James and J. M. Tour, *Adv. Mater.*, 2012, **24**, 4924-4955.
9 G. Eda and M. Chhowalla, *Adv. Mater.*, 2010, **22**, 2392-2415.
10 L. G. Guex, B. Sacchi, K. F. Peuvot, R. L. Andersson, A. M. Pourrahimi, V. Strom, S. Farris and R. T. Olsson, *Nanoscale*, 2017, **9**, 9562-9571.
11 S. Eigler and A. Hirsch, *Angew. Chem. Int. Ed.*, 2014, **53**, 7720-7738.
12 V. Georgakilas, J. N. Tiwari, K. C. Kemp, J. A. Perman, A. B. Bourlinos, K. S. Kim and R. Zboril, *Chem. Rev.*, 2016, **116**, 5464-5519.
13 R. K. Singh, R. Kumar and D. P. Singh, *RSC Adv.*, 2016, **6**, 64993-65011.
14 X. Yu, H. Cheng, M. Zhang, Y. Zhao, L. Qu and G. Shi, *Nat. Rev. Mater.*, 2017, **2**, 17046.
15 S. Eigler, *Chem.-Eur. J.*, 2016, **22**, 7012-7027.
16 P. P. Brisebois and M. Siaj, *J. Mater. Chem. C*, 2020, **8**, 1517-1547.
17 Q. Zheng, Z. Li, J. Yang and J.-K. Kim, *Prog. Mater. Sci.*, 2014, **64**, 200-247.
18 Z. U. Khan, A. Kausar, H. Ullah, A. Badshah and W. U. Khan, *J. Plast. Film Sheet.*, 2016, **32**, 336-379.
19 F. Meng, W. Lu, Q. Li, J. H. Byun, Y. Oh and T. W. Chou, *Adv. Mater.*, 2015, **27**, 5113-5131.
20 G. Gorgolis and C. Galiotis, *2D Mater.*, 2017, **4**, 032001.
21 K. Thakur and B. Kandasubramanian, *J. Chem. Eng. Data*, 2019, **64**, 833-867.
22 R. K. Joshi, S. Alwarappan, M. Yoshimura, V. Sahajwalla and Y. Nishina, *Appl. Mater. Today*, 2015, **1**, 1-12.
23 Q. Ke and J. Wang, *J. Materiomics*, 2016, **2**, 37-54.
24 W. K. Chee, H. N. Lim, Z. Zainal, N. M. Huang, I. Harrison and Y. Andou, *J. Phys. Chem. C*, 2016, **120**, 4153-4172.
25 J. Liu, Z. Liu, C. J. Barrow and W. Yang, *Anal. Chim. Acta*, 2015, **859**, 1-19.
26 Q. Mei, B. Liu, G. Han, R. Liu, M. Y. Han and Z. Zhang, *Adv. Sci.*, 2019, **6**, 1900855.
27 G. Kucinskis, G. Bajars and J. Kleperis, *J. Power Sources*, 2013, **240**, 66-79.
28 R. Yadav, A. Subhash, N. Chemmenchery and B. Kandasubramanian, *Ind. Eng. Chem. Res.*, 2018, **57**, 9333-9350.
29 M. Daniyal, B. Liu and W. Wang, *Curr. Med. Chem.*, 2019, DOI: 10.2174/1381612825666190201129629O.
30 R. Narayan, J. E. Kim, J. Y. Kim, K. E. Lee and S. O. Kim, *Adv. Mater.*, 2016, **28**, 3045-3068.
31 W. K. Chee, H. N. Lim, N. M. Huang and I. Harrison, *RSC Adv.*, 2015, **5**, 68014-68051.
32 C. Schafhaeutl, *J. Prakt. Chem.*, 1840, **21**, 129-157.
33 B. C. Brodie, *Ann. Chim. Phys.*, 1855, **45**, 351-353.
34 L. Staudenmaier, *Ber.*, 1898, **31**, 1481-1487.
35 L. Staudenmaier, *Ber.*, 1899, **32**, 1394-1399.
36 G. Charpy, *C. R. Acad. Sci.*, 1909, **148**, 920-923.
37 U. Hofmann and E. König, *Z. Anorg. Allg. Chem.*, 1937, **234**, 311-336.
38 W. S. Hummers and R. E. Offeman, *J. Am. Chem. Soc.*, 1958, **80**, 1339.
39 A. Lerf, H. He, M. Forster and J. Klinowski, *J. Phys. Chem. B*, 1998, **102**, 4477-4482.
40 W. Cai, R. D. Piner, F. J. Stadermann, S. Park, M. A. Shaibat, Y. Ishii, D. Yang, A. Velamakanni, S. J. An, M. Stoller, J. An, D. Chen and R. S. Ruoff, *Science*, 2008, **321**, 1815-1817.
41 L. B. Casabianca, M. A. Shaibat, W. W. Cai, S. Park, R. Piner, R. S. Ruoff and Y. Ishii, *J. Am. Chem. Soc.*, 2010, **132**, 5672-5676.
42 L. Yang, R. Zhang, B. Liu, J. Wang, S. Wang, M. Y. Han and Z. Zhang, *Angew. Chem. Int. Ed.*, 2014, **53**, 10109-10113.
43 H. Pieper, S. Chercheja, S. Eigler, C. E. Halbig, M. R. Filipovic and A. Mokhir, *Angew. Chem. Int. Ed.*, 2016, **55**, 405-407.
44 A. Dimiev, D. V. Kosynkin, L. B. Alemany, P. Chaguine and J. M. Tour, *J. Am. Chem. Soc.*, 2012, **134**, 2815-2822.
45 A. M. Dimiev, L. B. Alemany and J. M. Tour, *ACS Nano*, 2013, **7**, 576-588.
46 A. M. Dimiev, L. B. Alemany and J. M. Tour, *ACS Nano*, 2012, **7**, 576-588.
47 A. Naumov, F. Grote, M. Overgaard, A. Roth, C. E. Halbig, K. Norgaard, D. M. Guldi and S. Eigler, *J. Am. Chem. Soc.*, 2016, **138**, 11445-11448.
48 J. P. Rourke, P. A. Pandey, J. J. Moore, M. Bates, I. A. Kinloch, R. J. Young and N. R. Wilson, *Angew. Chem. Int. Ed.*, 2011, **50**, 3173-3177.
49 N. V. Kozhemyakina, S. Eigler, R. E. Dinnebier, A. Inayat, W. Schwieger and A. Hirsch, *Fuller. Nanotub. Car. N.*, 2013, **21**, 804-823.
50 J. Walter, T. J. Nacken, C. Damm, T. Thajudeen, S. Eigler and W. Peukert, *Small*, 2015, **11**, 814-825.
51 C. E. Halbig, T. J. Nacken, J. Walter, C. Damm, S. Eigler and W. Peukert, *Carbon*, 2016, **96**, 897-903.

52 T. J. Nacken, C. E. Halbig, S. E. Wawra, C. Damm, S. Romeis, J. Walter, M. J. Tehrani, Y. C. Hu, Y. Ishii, S. Eigler and W. Peukert, *Carbon*, 2017, **125**, 360-369.
53 W. Rüdorff and U. Hofmann, *Z. Anorg. Allg. Chem.*, 1938, **238**, 1-50.
54 S. Seiler, C. E. Halbig, F. Grote, P. Rietsch, F. Borrnert, U. Kaiser, B. Meyer and S. Eigler, *Nat. Commun.*, 2018, **9**, 836.
55 A. M. Dimiev, G. Ceriotti, N. Behabtu, D. Zakhidov, M. Pasquali, R. Saito and J. M. Tour, *ACS Nano*, 2013, **7**, 2773-2780.
56 A. Lerf, *Daton Trans.*, 2014, **43**, 10276-10291.
57 J. O. Besenhard and H. P. Fritz, *Angew. Chem. Int. Ed.*, 1983, **22**, 950-975.
58 R. Nishitani, Y. Sasaki and Y. Nishina, *Synth. Met.*, 1989, **34**, 315-321.
59 N. Morimoto, H. Suzuki, Y. Takeuchi, S. Kawaguchi, M. Kunisu, C. W. Bielawski and Y. Nishina, *Chem. Mater.*, 2017, **29**, 2150-2156.
60 S. Eigler, C. Dotzer and A. Hirsch, *Carbon*, 2012, **50**, 3666-3673.
61 S. Eigler, M. Enzelberger-Heim, S. Grimm, P. Hofmann, W. Kroener, A. Geworski, C. Dotzer, M. Rockert, J. Xiao, C. Papp, O. Lytken, H. P. Steinrück, P. Müller and A. Hirsch, *Adv. Mater.*, 2013, **25**, 3583-3587.
62 S. Pei, Q. Wei, K. Huang, H. M. Cheng and W. Ren, *Nat. Commun.*, 2018, **9**, 145.
63 P. Feicht, J. Biskupek, T. E. Gorelik, J. Renner, C. E. Halbig, M. Maranska, F. Puchtler, U. Kaiser and S. Eigler, *Chem.-Eur. J.*, 2019, **25**, 8955-8959.
64 A. T. Smith, A. M. LaChance, S. Zeng, B. Liu and L. Sun, *Nano Mater. Sci.*, 2019, **1**, 31-47.
65 F. Pendolino, G. Capurso, A. Maddalena and S. Lo Russo, *RSC Adv.*, 2014, **4**, 32914-32917.
66 G. Ceriotti, A. Y. Romanchuk, A. S. Slesarev and S. N. Kalmykov, *RSC Adv.*, 2015, **5**, 50365-50371.
67 L. G. Cançado, A. Jorio, E. H. M. Ferreira, F. Stavale, C. A. Achete, R. B. Capaz, M. V. O. Moutinho, A. Lombardo, T. S. Kulmala and A. C. Ferrari, *Nano Lett.*, 2011, **11**, 3190-3196.
68 M. M. Lucchese, F. Stavale, E. H. M. Ferreira, C. Vilani, M. V. O. Moutinho, R. B. Capaz, C. A. Achete and A. Jorio, *Carbon*, 2010, **48**, 1592-1597.
69 L. Wang, A. Ambrosi and M. Pumera, *Angew. Chem. Int. Ed.*, 2013, **52**, 13818-13821.
70 Z. Wang, Q. Yao and S. Eigler, *Chem.-Eur. J.*, 2019, DOI: 10.1002/chem.201905252.
71 J. M. Englert, P. Vecera, K. C. Knirsch, R. A. Schafer, F. Hauke and A. Hirsch, *ACS Nano*, 2013, **7**, 5472-5482.
72 S. Eigler, F. Hof, M. Enzelberger-Heim, S. Grimm, P. Müller and A. Hirsch, *J. Phys. Chem. C*, 2014, **118**, 7698-7704.
73 P. Vecera, S. Eigler, M. Kolesnik-Gray, V. Krstic, A. Vierck, J. Maultzsch, R. A. Schafer, F. Hauke and A. Hirsch, *Sci. Rep.*, 2017, **7**, 45165
74 F. Grote, C. Gruber, F. Borrnert, U. Kaiser and S. Eigler, *Angew. Chem. Int. Ed.*, 2017, **56**, 9222-9225.
75 B. D. L. Campéon, M. Akada, M. S. Ahmad, Y. Nishikawa, K. Gotoh and Y. Nishina, *Carbon*, 2020, **158**, 356-363.
76 A. M. Abdelkader, A. J. Cooper, R. A. Dryfe and I. A. Kinloch, *Nanoscale*, 2015, **7**, 6944-6956.
77 Z. Y. Xia, S. Pezzini, E. Treossi, G. Giambastiani, F. Corticelli, V. Morandi, A. Zanelli, V. Bellani and V. Palermo, *Adv. Func. Mater.*, 2013, **23**, 4684-4469.
78 H. Thiele, *Z. Elektrochem.*, 1934, **40**, 26-33.
79 H. Thiele, *Z. Anorg. Allg. Chem.*, 1932, **206**, 407-415.
80 K. Parvez, R. Li, S. R. Puniredd, Y. Hernandez, F. Hinkel, S. Wang, X. Feng and K. Müllen, *ACS Nano*, 2013, **7**, 3598-3606.
81 Z. Xia, G. Maccaferri, C. Zanardi, M. Christian, L. Ortolani, V. Morandi, V. Bellani, A. Kovtun, S. Dell'Elce, A. Candini, A. Liscio and V. Palermo, *J. Phys. Chem. C*, 2019, **123**, 15122-15130.
82 S. Eigler, C. Dotzer, F. Hof, W. Bauer and A. Hirsch, *Chem.-Eur. J.*, 2013, **19**, 9490-9496.
83 S. Eigler, S. Grimm, F. Hof and A. Hirsch, *J. Mater. Chem. A*, 2013, **1**, 11559-11562.
84 H. Pieper, C. E. Halbig, L. Kovbasyuk, M. R. Filipovic, S. Eigler and A. Mokhir, *Chem.-Eur. J.*, 2016, **22**, 15389-15395.
85 A. M. Dimiev and T. A. Polson, *Carbon*, 2015, **93**, 544-554.
86 M. Ghorbani, H. Abdizadeh and M. R. Golobostanfard, *Proc. Mater. Sci.*, 2015, **11**, 326-330.
87 R. Tang, K. Taguchi, H. Nishihara, T. Ishii, E. Morallón, D. Cazorla-Amorós, T. Asada, N. Kobayashi, Y. Muramatsu and T. Kyotani, *J. Mater. Chem. A*, 2019, **7**, 7480-7488.
88 I. A. Vacchi, C. Spinato, J. Raya, A. Bianco and C. Menard-Moyon, *Nanoscale*, 2016, **8**, 13714-13721.
89 R. Khan, R. Nakagawa, B. Campeon and Y. Nishina, *ACS Appl. Mater. Interfaces*, 2020, DOI: 10.1021/acsami.9b21082.

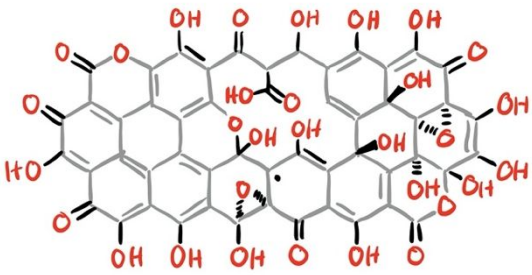

This is a tutorial review based on laboratory experience on the synthesis of graphene oxide using chemical and electrochemical methods.